DLR Falcon Dropsonde Operation in T-PARC and Analysis of the Environment Surrounding Typhoons

Kotaro Bessho[1], Tetsuo Nakazawa[1] and Martin Weissmann[2]

[1] Meteorological Research Institute, Japan Meteorological Agency
[2] German Aerospace Center, Oberpfaffenhofen, Germany

1. DLR Falcon dropsonde operation in T-PARC

From 23 August to 4 October 2008, missions of the German Aerospace Center (DLR)'s Falcon 20-E5 aircraft (Figure 1) were executed under T-PARC in conjunction with the Meteorological Research Institute of the Japan Meteorological Agency. In terms of observational equipment, the aircraft used a dropsonde system, wind lidar, moisture profile lidar of DIAL in T-PARC. On observational flights, the Falcon was manned by two pilots, an engineer and three researchers. The plane's maximum flight range is 1,500 nautical miles (corresponding to around four hours of flight time), and its maximum flight altitude is FL390 – almost 200 hPa. Its dropsonde system, manufactured by Vaisala, has four channels in its receiver and can observe the overall atmospheric profile once every five minutes. The observational data collected by the Falcon were submitted to the WMO GTS via satellite phone through the Iridium system in the T-PARC mission. The Falcon used the US Naval Air Facility Atsugi as its main airport, and sometimes stopped at the US bases in Misawa, Iwakuni and Kadena (Figure 2) to refuel and for overnight stays.

Figure 1 The DLR Falcon 20-E5 (© The Yomiuri Shimbun)

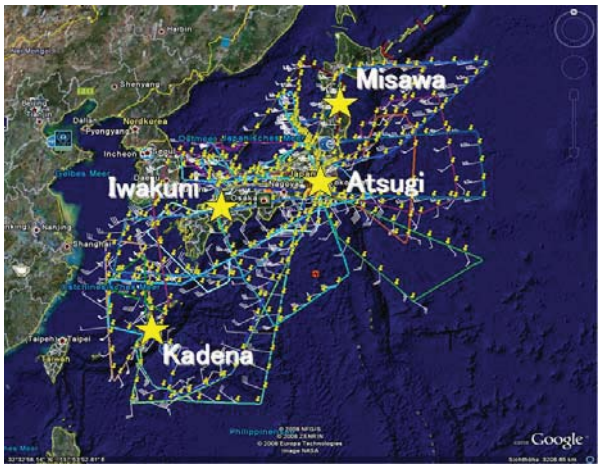

Figure 2　All Falcon flight paths in T-PARC

The Falcon observed atmospheric profiles inside and outside cloud masses surrounding typhoons using its dropsonde system, engaging in 25 missions around the Japanese islands over a total flight time of 85 hours (Table 1). The total number of dropsondes employed on these flights was 328. The observational targets were mainly the recurvatures and extratropical cyclone transitions of typhoons Sinlaku and Jangmi.

Table 1　Summary of Falcon missions in T-PARC including flight mission numbers, take-off/landing bases, start dates, flight times, block times, dropsonde numbers, mission types and target systems

Flight	Location		Start Date	Flight Time					Block Time	Drops.	Type	System
				LT		UTC						
	from	to	Atsugi	Start	End	Start	End	Duration	Duration			
0	DLR OP	DLR OP							1:30:00	0	test flight	---
1	Atsugi	Atsugi	2008/8/26	7:20	10:55	22:20	1:55	3:35:00	3:50:00	9	T, RB	
2	Atsugi	Atsugi	2008/8/30	7:10	10:35	22:10	1:35	3:25:00	3:40:00	15	TWE, ET	TCS25
3	Atsugi	Atsugi	2008/8/31	7:10	10:55	22:10	2:05	3:55:00	4:10:00	16	TWE, ET	TCS26
4	Atsugi	Atsugi	2008/9/2	7:20	10:50	22:20	1:50	3:30:00	3:45:00	17	midlat T	
5	Atsugi	Atsugi	2008/9/4	6:55	10:35	21:55	1:35	3:40:00	3:55:00	15	midlat T	
6	Atsugi	Atsugi	2008/9/9	7:10	10:50	22:10	1:50	3:40:00	3:55:00	18	T, ET	TCS37
7	Atsugi	Kadena	2008/9/11	12:20	16:20	3:20	7:20	4:00:00	4:00:00	19	Typhoon	Sinlaku
8	Kadena	Atsugi		17:15	21:20	8:15	12:20	4:05:00	4:20:00	17	Typhoon	Sinlaku
9	Atsugi	Iwa-Kuni	2008/9/14	8:30	12:45	23:30	3:15	3:45:00	4:00:00	22	Typhoon	Sinlaku
10	Iwa-Kuni	Atsugi		13:45	14:55	4:45	5:55	1:10:00	1:25:00	0	Typhoon	Sinlaku
11	Atsugi	Kadena	2008/9/16	6:35	10:20	21:35	1:20	3:45:00	4:00:00	17	Typhoon	Sinlaku
12	Kadena	Atsugi		14:00	17:00	5:00	8:00	3:00:00	3:50:00	3	Typhoon	Sinlaku
13	Atsugi	Iwa-Kuni	2008/9/17	12:20	15:35	3:20	6:35	3:15:00	3:30:00	17	ET	Sinlaku
14	Iwa-Kuni	Atsugi		16:50	20:15	7:50	11:15	3:25:00	3:40:00	15	ET	Sinlaku
15	Atsugi	Atsugi	2008/9/18	12:25	16:20	3:25	7:20	3:45:00	4:10:00	16	ET	Sinlaku
16	Atsugi	Misawa	2008/9/19	7:35	8:55	22:35	23:55	1:20:00	1:35:00	3	ET	Sinlaku
17	Misawa	Atsugi		10:10	14:10	1:10	5:10	4:00:00	4:15:00	19	ET	Sinlaku
18	Atsugi	Atsugi	2008/9/21	7:05	11:05	22:05	2:05	4:00:00	4:15:00	12	ET	Sinlaku
19	Atsugi	Kadena	2008/9/28	12:10	16:00	3:10	7:00	3:50:00	4:05:00	13	Typhoon	Jangmi
20	Kadena	Kadena		17:45	19:50	8:45	11:10	2:25:00	2:40:00	9	Typhoon	Jangmi
21	Kadena	Kadena	2008/9/29	12:45	16:15	3:45	7:15	3:50:00	4:05:00	10	Typhoon	Jangmi
22	Kadena	Atsugi	2008/9/30	7:10	10:40	22:10	1:40	3:30:00	3:45:00	12	ET, T	Jangmi
23	Atsugi	Atsugi		12:55	17:50	3:55	8:50	3:55:00	4:10:00	8	ET, T	Jangmi
24	Atsugi	Iwa-Kuni	2008/10/1	14:15	17:30	5:15	8:30	3:15:00	3:30:00	16	ET	Jangmi
25	Iwa-Kuni	Atsugi		19:45	22:30	10:45	13:30	2:45:00	3:00:00	10	Typhoon	Jangmi
								84:45:00	93:00:00	328		

Three other aircraft were used on T-PARC missions, including the USAF Hurricane Hunters WC-130 and the NRL P-3. Since the main targets of these two planes were typhoon genesis and recurvature, they used Guam as their main airport. The other aircraft was the DOTSTAR program's Astra, which flew near Taiwan Island to cover the typhoon recurvature stage. All three were equipped with dropsonde systems to enable atmospheric profiling in areas near typhoons. In particular, the WC-130 also sometimes executed eye-wall penetration flights. The total number of flight hours logged in T-PARC by the four aircraft including the Falcon was more than 500 over 76 missions.

2. Autumn rain front and typhoons

In late summer and early autumn, the Autumn Rain Front (ARF) approaches the Japanese islands. The ARF is similar to the Baiu-Meiyu-Chagma front in early summer, but usually it brings light rain rather than the heavy rainfall of the Baiu front. It is usually located near the Japanese islands with an east-west orientation, and sometimes causes major disasters such as flash flooding in combination with typhoons moving to mid-latitude areas. By way of example, the torrential rain in the Tokai region observed in Nagoya City (located in the central part of Japan's main island) from 11 to 12 September 2000 was caused by interaction between the ARF and Typhoon Saomai (0014) (Kitabatake 2002).

As mentioned above, the combination of the ARF with typhoon conditions sometimes brings major disasters to the Japanese islands. Many field experiments and research projects have been carried out in regard to the Baiu front, and special observations of it prove successful if the monitoring period is long enough. However, there has been a lack of research involving observational experiments for the ARF because of the extreme difficulty and risk involved in capturing the rare cases of heavy ARF rainfall in combination with typhoons. In T-PARC, the Falcon had many chances for detailed observation of ARF structures under the influence of typhoons. In such conditions, the ARF may produce extensive latent heat release, thereby changing the structure of the typhoon itself. Accordingly, it is very important to analyze such fronts observationally. In the next section, typical results of ARF observation from a Falcon dropsonde mission will be shown to allow analysis of the environmental structure of typhoons.

3. ARF case study

Below are some results of observing the ARF under the influence of a typhoon approaching the Japanese islands. Figure 3 is a JMA surface weather map made with data from 00 UTC on 16 September 2008. From this figure, it can be understood that Typhoon Sinlaku (0813) was positioned north of Taiwan Island, with the ARF located along the southern coast of Japan's main islands. Figure 4 shows an MTSAT infrared satellite image taken at the same time as the data used for the weather map. The red dots with numbers represent the dropsonde observational points of the Falcon, and the yellow stars show the two JMA operational upper-sounding sites used in the analysis.

Dropsonde observation was executed from 2207 UTC on 15 September to 0106 UTC on 16 September. Figure 5 shows a rain intensity image for the area over the Japanese islands retrieved from JMA's operational radars at 2200 UTC on 15 September. From these figures, it can be seen that the dropsonde observational points and JMA's upper-sounding sites were located over the ARF in a north-to-south direction.

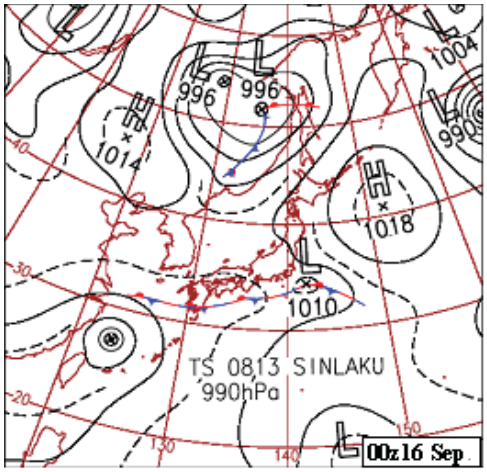

Figure 3 JMA surface weather map for 00 UTC on 16 September 2008

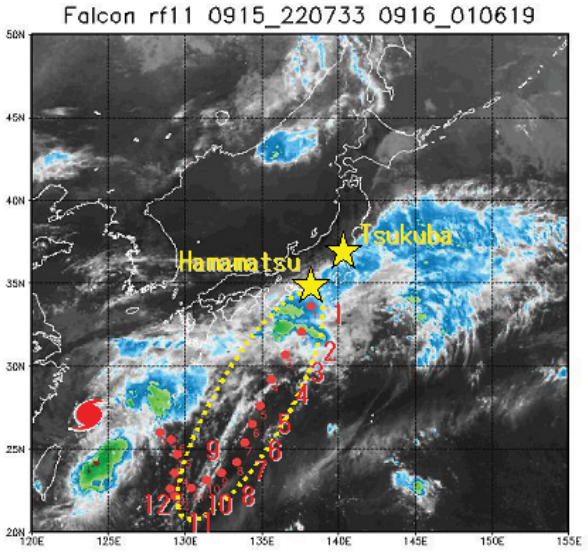

Figure 4 Infrared image from MTSAT-1R at 00 UTC on 16 September 2008. The red dots show Falcon dropsonde observational points, and the yellow stars indicate the JMA operational upper-sounding sites used in the analysis.

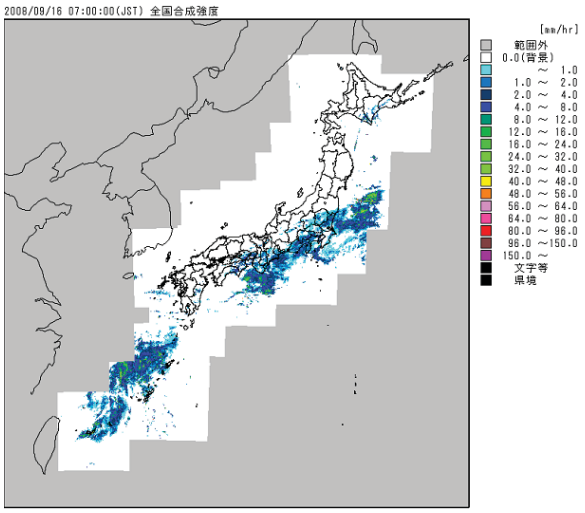

Figure 5 Rain intensity (mm/hr) as retrieved from JMA operational radars at 2200 UTC on 15 September 2008

Figure 6 shows cross sections derived from atmospheric profiles of dropsondes #1 – 12 and two operational soundings at Tsukuba and Hamamatsu. Tsukuba was located to the north of the ARF, Hamamatsu and dropsondes #1 – 3 were located within it, and dropsondes #4 – 12 were to its southern side. Figures 6 (a), (b) and (c) show cross sections of potential temperature, specific humidity and equivalent potential temperature, respectively, with each indicating the same cross section of horizontal wind. In this case study, the lower structure of the ARF below 950 hPa was the point of focus.

At Tsukuba, the horizontal wind had an easterly component, but it was very weak at a lower level. At Hamamatsu, the wind speed showed a sudden increase to almost 10 m/s. The horizontal wind at dropsonde #1 had almost the same speed, but its direction was northeasterly. Unfortunately, no wind data were obtained from dropsonde #2. At dropsonde #3 located to the southern edge of the ARF, the wind speed was 5 m/s and its direction was southwesterly. From the wind speeds and directions between dropsondes #1 and #3, it can be easily inferred that there is a strong convergence within the ARF at a lower level. Wind data for dropsondes #4 and #5 are also missing. At dropsonde #6, the wind speed was almost 5 m/s, and its direction was southeasterly. The horizontal winds at dropsondes #7 – 12 were very weak (below 700 hPa).

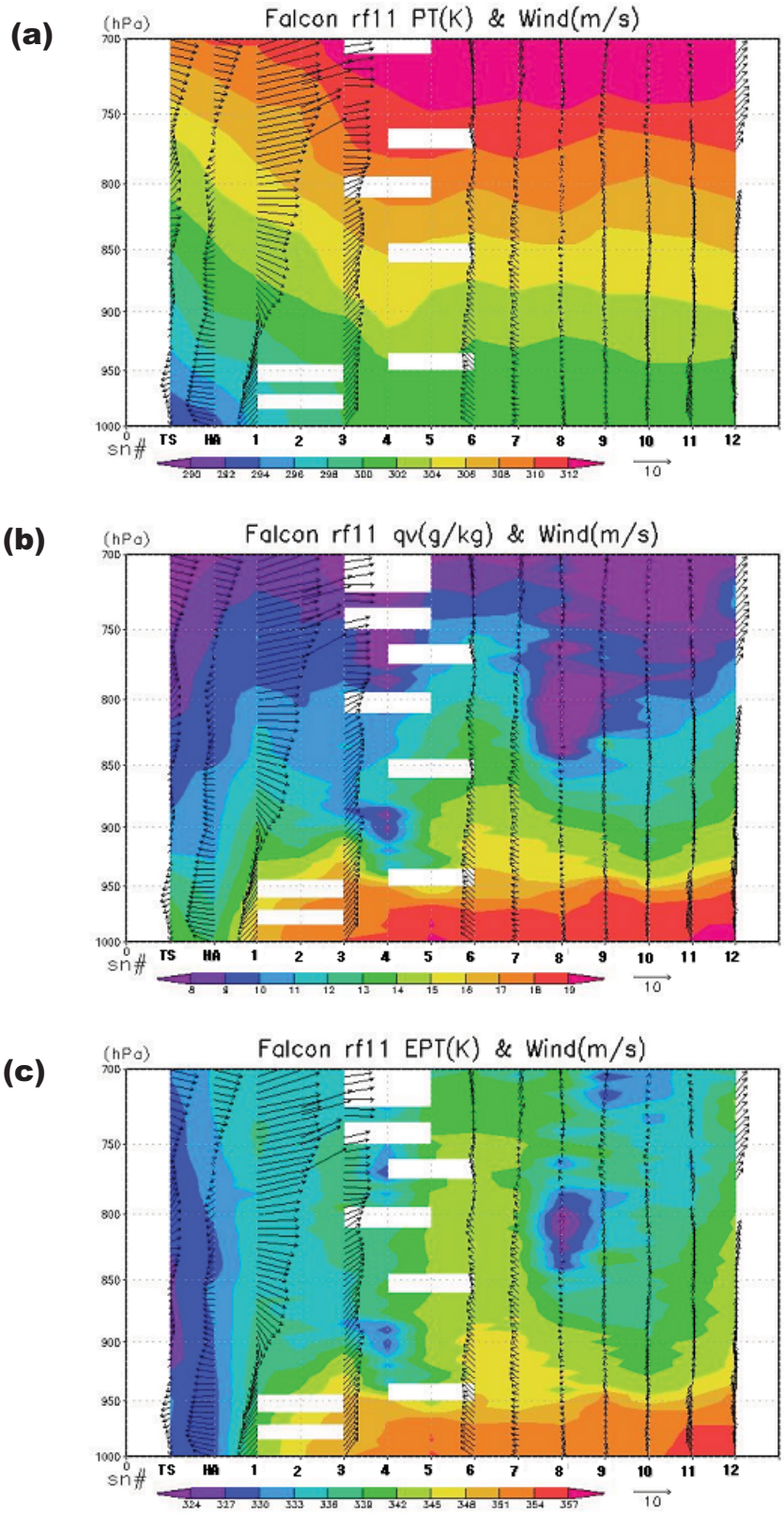

Figure 6　Cross sections derived using atmospheric profiles from dropsondes #1 – 12 and two operational soundings at Tsukuba (TS) and Hamamatsu (HA).　(a) Potential temperature (K); (b) specific humidity (g/kg); (c) equivalent potential temperature (K).　(a) – (c) also include horizontal wind vectors (m/s).

For the potential temperature profile at the lowest level, there was a significant gradient between Tsukuba and dropsonde #3 corresponding to the ARF itself (Figure 6 (a)). The gradient of potential temperatures below 950 hPa over the southern side of the ARF was very small, while the horizontal distribution of specific humidity showed a large gradient between Tsukuba and dropsonde #4 (Figure 6 (b)). Reflecting the distribution of potential temperature and specific humidity at the lowest level, the horizontal gradient of equivalent potential temperature at this level between Hamamatsu and dropsonde #4 was very large, and the level of stability over these areas was almost neutral (Figure 6 (c)). On the other hand, the gradient of equivalent potential temperature between dropsondes #4 and #10 was very weak, and the equivalent potential temperature was high at the lowest level and low above 950 hPa. This indicates that the southern side of the ARF was in a state of convective instability. In conclusion, it was found that the southern side of the ARF was characterized by a horizontal atmospheric structure with a small gradient of potential temperature and a large gradient of specific humidity.

This structure of the southern ARF appears to be similar to that of the Baiu front as found by Moteki et al. (2006), who executed dropsonde observation using aircraft on the Baiu front and showed a strong temperature gradient within the front itself and a strong humidity gradient over its southern side. In their paper, this strong moisture gradient was called a water vapor front. From our analysis, it can be concluded that there is also a water vapor front over the southern side of the ARF, which has a structure similar to that of the Baiu front.

References

Kitabatake, N., 2002: The role of convective instability and frontogenetic circulation in the torrential rainfall in the Tokai District on 11-12 September 2000. *Pap. Met. Geophys.*, **53**, 91-108 (in Japanese).

Moteki, Q., T. Shinoda, S. Shimizu, S. Maeda, H. Minda, K. Tsuboki and H. Uyeda, 2006: Multiple Frontal Structures in the Baiu Frontal Zone Observed by Aircraft on 27 June 2004. SOLA, **2**, 132-135.